Molecular Dynamics Simulation Studies of Zeolite-A. I. Structure and Dynamics of Na^+ Ions in Rigid Dehydrated Zeolite-A Framework

Gyeong Keun Moon, Sang Gu Choi†, Han Soo Kim‡, and Song Hi Lee*

Department of Chemistry, Kyungsung University, Pusan 608-736
†Department of Industrial Safety, Yangsan Junior College, Yangsan 626-800
‡Daesung Cryogenic Research Institute, Daesung Sanso Co., Ansan 425-090. *Received February 13, 1992*

Structure and dynamics of Na^+ ions are investigated by molecular dynamics simulations of rigid dehydrated zeolite-A at several temperatures using a simple Lennard-Jones potential plus Coulomb potential. A best-fitted set of electrostatic charges is chosen from the results of simulation at 298.15 K and Ewald summation technique is used for the long-ranged character of Coulomb interaction. The calculated *x*, *y*, and *z* coordinates of Na^+ ions are in good agreement with the positions determined by X-ray crystallography within statistical errors, their random movings in different types of closed cages are well described by time-correlation functions, and Na_I type ions are found to be less diffusive than Na_{II} and Na_{III}. At 600.0 K, the unstable Na_{III} type ion pushes down one of nearest Na_I ions into the β-cage and sits on the stable site I, and the captured ion in the β-cage wanders over and attacks one of 8 Na_I type ions.

Introduction

Zeolites are microporous aluminoilicates with relatively rigid anionic frameworks which contain exchangeable cations and generally removable and replaceable guest molecules such as water and organic compounds. The framework of zeolite-A[1] is generated by placing a cubic double 4-ring units (D4R, $Al_4Si_4O_{16}$) in the centers of the edges of a cube of edge 12.3 A. This arrangement produces truncated octahedral units centered at the corners of the cube. Each corner of the cube is occupied by a truncated octahedron (β-cage) enclosing a cavity with a free diameter of 6.6 A. The center of the unit cell is a large cavity (α-cage) which has a free diameter of 11.4 A. Entry into the α-cage cavity is possible through six 16-membered $Al_4Si_4O_8$ rings (called 8-ring), mean free diameter of which is approximately 4.2 A. Each β-cage cavity is surrounded cubically by eight α-cage cavities and can be entered from each α-cage through a 2.2 A 12-membered $Al_3Si_3O_6$ 6-ring.

In dehydrated zeolite-A which is the system of interest in this paper, eight Na^+ ions, Na_I type, are displaced 0.21 A into the α-cage from the center of the 6-rings. Three Na^+ ions, Na_{II} type, are located in the 8-rings displaced about 1.3 A from the center. The Na_{II} type ions, by partial blocking of the aperture, influence the adsorption of gases and vapors and regulate the pore size. The remaining Na^+ ion, Na_{III} type, is located opposite to the 4-ring displaced approximately 1.73 A into the α-cage.[2] When exchanged by Ca^{2+} ions, 4 Ca^{2+} and 4 Na^+ ions consist of each unit cell, the eight site I positions are occupied ant the sites II and III positions are vacant[3] (this system is the second object in a series of our studies of zeolite-A). Consequently the apertures are completely open and capable of admitting molecules with diameters of about 4.2 A. Hydrated Zeolite-A contains 12 Na^+ ions and 28 (or 27) water molecules. Compared with the dehydrated one, only the Na_{III} type ion has a different position which is located at the center of the α-cage.[4] Four water molecules within the small β-cage apparently bond to the framework oxygens and form a distorted tetrahedral structure. It is only predicted that 20 water molecules form a distorted dodecahedral arrangement in the large α-cage[4] and even the number of water molecules in unit cell is not clearly determined. Because of controversy about the number and sturcture of water molecules in the α-cage of hydrated zeolite-A, we will study this system as the third object in the series of our studies of zeolite-A.

Computer calculation methods-energy minimization, molecular dynamics (MD) and Monte Carlo (MC) simulations-have become important techniques for the study of fluids, solids and adsorbed molecules in various zeolite systems. The first calculation on zeolite systems, based on simple potential energy minimizations, identified preferred adsorption sites or potential energy maps of the zeolite inner void space.[5-7] Later, MC simulations were employed to study the average siting of methane in zeolite Y[8] and in the zeolites ZSM-5 and mordenite.[9] Leherte *et al.*[10] studied concentration effects on water adsorption in ferrierite.

The advantage of MD over MC is that not only static but also dynamic properties can be obtained, so that most simulation works on zeolite systems have been studied by MD method. For example, Demontis and co-workers, by using simple model potentials, reproduced the positions and vibrations of water molecules in the cages of natrolite,[11,12] the atomic coordinates and the crystal symmetry of dehydrated natrolite[13] and Linde zeolite 4A,[14] and their dynamical behavior in their MD simulation works. Further studies of the group included the diffusive motion of methane in silicate[15] and the structural changes of silicate at different temperatures by a MD method.[16] Cohen de Lara and co-workers also performed a MD study of methane adsorbed in zeolite-A[17] based on their potential-energy calculation.[18] Other MD studies on time-dependent properties such as diffusion coefficients and intracrystalline site residence times were reported for methane in zeolite Y,[19] mordenite,[20] and ZSM-5,[20] for benzene in zeolite Y,[21] for water in ferrierite,[22-25] and for xenon,[26] methane, ethane, and propane in silicalite.[27] The dy-

namics of Na^+ ions inside a zeolite-A framework at several temperatures was described by a MD simulation by Shin *et al.*[28]

In this paper, we perform molecular dynamics (MD) simulation of Na^+ ions in dehydrated zeolite-A framework. The purpose of this work is three-fold: first, the determination of model potential parameters of Na^+ ions and framework atoms for this and further studies of zeolite-A systems and, second, the test of Ewald summation[29,30] technique which is very important for long-range interactions such as Coulomb potential, especially for infinite three-dimensional crystalline structures like zeolites. The successful use of Ewald summation in MD simulations was reported in the study of water in ferrierite by Leherte *et al.*[23-25] while Shin *et al.*[28] reported the inadequacy of Ewald summation in MD simulation of Na^+ ions in dehydrated zeolite-A, used a kind of switching function[31-33] instead, and concluded that the dynamic properrty of Na^+ ions in zeolite-A framework is not sensitive to the long-range electrostatic forces. Third, using the best-fitted interaction potentials and the Ewald summation technique, we want to re-examine the structure and dynamics of Na^+ ions in dehydrated zeolite-A at several temperatures.

In Section II, the details of molecular model and MD simulation methods are presented. We discuss the simulation results-energetics, structure, and dynamics of Na^+ ions-in Section III and present the concluding remarks in Section IV.

Molecular Models and Molecular Dynamics Simulation

Molecular Models. Zeolite-A framework is modelled by the pseudo cell, $(SiAlO_4)_{12}$, or the the $Pm\bar{3}m$ space group (a=12.2775 A) which contains 12 Na^+ ions. The framework is assumed to be rigid and the framework atoms are fixed in the space at the positions determied by X-ray diffraction experiment of Pluth and Smith[2] for the dehydrated zeolite-A system. Rigid framework simulations were carried out by Leherte *et al.*[22-25] on the diffusion of water in ferrierite, by Shin *et al.*[28] on the dynamics of Na^+ ions in dehydrated zeolite-A, and by Yashonath *et al.*[19] on the mobility of methane in zeolite Y, which was also studied by Monte Carlo method.[8] Na^+ ions are distributed initially at the X-ray positions[2] and are free to move according to equations of motion of motion as the simulation time evolves.

We get our model potential for Na^+ ions and framework atoms from Lennard-Jones (LJ) and Coulomb potentials for Na^+ ions and framework atoms from Lennard-Jones (LJ) and Coulom potential. One is short-ranged and the other is long-ranged for which an Ewald summations is used. Taking into account the framework heterogeneity, the total interaction potential of the system is modelled as a sum of pair-additive potentials between Na^+ ions themselves and between Na^+ ion i and each framework atom j:

$$\Phi=\sum_{i<j}^{ion}\sum\phi_{ij}+\sum_{i}^{ion}\sum_{j}^{frame}\phi_{ij} \tag{1}$$

where the interaction energy, ϕ_{ij}, is expressed

$$\phi_{ij}=4\varepsilon\left(\frac{\sigma^{12}}{r^{12}}-\frac{\sigma^{6}}{r^{6}}\right)+\frac{q_iq_j}{r} \tag{2}$$

whith $r=r_{ij}$. The LJ parameters ε and σ for Na^+ ions and framework atoms are given in Table 1, but the electrostatic charges q_i, on them are determined by comparing the simulation results of different values of q_{Na^+}, and q_{atom}'s which are calculated by using Huheey's electronegativity set[34] and Sanderson's electronegativity equalization principe.[35]

Ewald Summation. The charge-charge potential energy without Ewald summation is given as the second term of the right-hand side Eq. (2) and the force equation can be simply derived by $F_{ij}=-\nabla\phi_{ij}$. The corresponding equations with Ewald summation are, however, much complicated (see Ref. 36 for Ewald summation of dipolar system). Each equation splits into the sum of two parts, one in real space and the other in reciprocal space. The potential energies between Na^+ ions and between Na^+ ion and framework atom, and the force on Na^+ ion, in the real space, are given by

$$\phi_{i-i}^{real}=\frac{1}{2}\sum_{i\neq j}^{ion}\sum^{ion}q_iq_j\frac{erfc(\alpha r/L)}{r} \tag{3}$$

$$\phi_{i-f}^{real}=\frac{1}{2}\sum_{i}^{ion}\sum_{j}^{frame}q_iq_j\frac{erfc(\alpha r/L)}{r} \tag{4}$$

$$\mathbf{F}_i^{real}=\sum_{j\neq i}^{ion}\frac{1}{L^2}q_iq_j\left(\frac{2\alpha\exp[-(\alpha r/L)^2]}{\sqrt{\pi}(r/L)^2}+\frac{erfc(\alpha r/L)}{(r/L)^3}\right)\frac{\mathbf{r}}{L}+\sum_{j}^{frame}\frac{1}{L^2}q_iq_j\left(\frac{2\alpha\exp[-(\alpha r/L)^2]}{\sqrt{\pi}(r/L)^2}+\frac{erfc(\alpha r/L)}{(r/L)^3}\right)\frac{\mathbf{r}}{L} \tag{5}$$

where $r=|\mathbf{r}|$ with $\mathbf{r}=\mathbf{r}_{ij}=\mathbf{r}_i-\mathbf{r}_j$, L is the length of the simulation box, and $erfc(x)$ is the complementary error function. Eqs. (3) and (4) exclude the self-energy of the charge distribution.[30] The parameter α and the integer coordinates $n=(n_x, n_y, n_z)$ are chosen in such a way that a high accuracy of calculation is combined with a minimum of computing time. In the real space we consider only $n=(0, 0, 0)$ since the contribution of the other n's are vanishingly small. Letting $\alpha=0$ in Eqs. (3)-(5), we recover the equations without the Ewald summation.

The potential energies between Na^+ ions and between Na^+ ion and framework atom, and the force on Na^+ ion, in the reciprocal space, are given by

$$\phi_{i-i}^{rcpr}=\frac{1}{2\pi L}\sum_{n\neq 0}f(n)\left(\sum_{i}^{ion}q_i\cos(2\pi\mathbf{n}\cdot\mathbf{r}_i/L)\right)^2+\left(-\sum_{i}^{ion}q_i\sin(2\pi\mathbf{n}\cdot\mathbf{r}_i/L)\right)^2 \tag{6}$$

$$\phi_{i-f}^{rcpr}=\frac{1}{2\pi L}\sum_{n\neq 0}f(n)\left(\sum_{i}^{ion}q_i\cos(2\pi\mathbf{n}\cdot\mathbf{r}_i/L)\sum_{j}^{frame}q_j\cos(2\pi\mathbf{n}\cdot\mathbf{r}_j/L)+\sum_{i}^{ion}q_i\sin(2\pi\mathbf{n}\cdot\mathbf{r}_i/L)\sum_{j}^{frame}q_j\sin(2\pi\mathbf{n}\cdot\mathbf{r}_j/L)\right) \tag{7}$$

$$\begin{aligned}\mathbf{F}_i^{rcpr}=\frac{2}{L^2}\sum_{n\neq 0}f(n)\mathbf{n}\Big(&q_i\sin(2\pi\mathbf{n}\cdot\mathbf{r}_i/L)\sum_{j=1}^{ion}q_j\cos(2\pi\mathbf{n}\cdot\mathbf{r}_j/L)\\&-q_i\cos(2\pi\mathbf{n}\cdot\mathbf{r}_i/L)\sum_{j=1}^{ion}q_j\sin(2\pi\mathbf{n}\cdot\mathbf{r}_j/L)\\&+q_i\sin(2\pi\mathbf{n}\cdot\mathbf{r}_i/L)\sum_{j}^{frame}q_j\cos(2\pi\mathbf{n}\cdot\mathbf{r}_j/L)\\&-q_i\cos(2\pi\mathbf{n}\cdot\mathbf{r}_i/L)\sum_{j}^{frame}q_j\sin(2\pi\mathbf{n}\cdot\mathbf{r}_j/L)\Big)\end{aligned} \tag{8}$$

were

$$f(n)=\exp[-(\pi n/\alpha)^2]/n^2 \quad (9)$$

and $n=|r|$. Letting $\alpha=0$ in $f(n)$ makes $f(n)=0$ leaving the terms in the reciprocal space equal to zero. In our simulation runs, the values of α and n_{max} are chosen as 3.0 and 5.0 from the review of previous works.[30,36]

Molecular Dynamics Simulation. The best choice for the simulation ensemble is certanly a canonical ensemble in which N (number of prticles), V (volume of zeolite), and T (temperature) are fixed. To maintain the system at a constant temperature, we use Guss's principle of least constraint[37] and the equations of motion for particle i are given by

$$\dot{r}_i=p_i/m \quad (10)$$

$$\dot{p}_i=F_i-\lambda p_i \quad (11)$$

where F_i is the force on particle i and the temperature constraint parameter λ is obtained by the substitution of $\dot{p}_i$ from Eq. (11) into the requiremnt, $\Sigma\dot{p}_i\cdot p_i=0$:

$$\lambda=\sum_i^N p_i\cdot F_i/\sum_i^N p_i^2 \quad (12)$$

The ordinary periodic boundary condition in the x-, y-, and z-directions and minimum image convention are applied for the LJ potential, but we consider only an interaction between each Na^+ ion and the nearest framework atom or its image without the use of cut-off distance. This results from the dominancy of the Coulomb interaction which is treated as the Ewald summation.

Gear's fifth order predictor corrector method[38] is used for the time integration of Eqs. (10) and (11). The time step used in the simulation runs is 2.00×10^{-16} sec. First simulation runs are used for the determination of the model potential parameters of Na^+ ions and framework atoms at 298.15 K. By using these potential parameters of the main NVT MD simulations for three different temperatures of 298.15, 100.0, and 600.0 K are carried out. Having done each simulation run of 50,000 time steps at least, the initial positions of Na^+ ions are broken down and the system comes to equilibrium state. We get the potential energies and positions of Na^+ ions by the mean value of another 50,000 time steps.

Results and Discussion

Electrostatic charges of the framework atoms, q_{atom}'s, for given several Na^+ ionic charges, q_{Na^+}, are calculated by using Huheey's electronegativity set[34], Sanderson's electronegativity equalization principle and electric neutrality principle.[35]

$$\sum_{i\neq Na^+} q_i=-q_{Na^+} \quad (13)$$

$$a_i+b_iq_i=a_j+b_jq_j, \qquad i,\ j\neq Na^+ \quad (14)$$

where a_i and b_i are the inherent electronegativity and the charge coefficient of atom i respectively, and i and j represent Si, Al, O_1, O_2, and O_3. The designation of the oxygen atoms, O_i's, is depends upon their site symmetries: O_1 is the member of 4-ring and 8-ring, O_2 of 6-ring and 8-ring, and O_3 of 4-ring and 6-ring. The calculated electrostatic charges are given in Table 2. In this work, the LJ parameters and the electrostatic charges on Si are assumed to be equal to those on Al, since the Ewald summation in the pseudo cell [$Pm3m$, $(SiAlO_4)_{12}$] is valid with this assumtion. Otherwise, in the case of different potential parameters of Al and Si, the true cell [$Fm3m$, $(SiAlO_4)_{96}$] should be used for the Ewald summation because of the symmetric property of zeolite-A. For simplicity, we have chosen the former cell system.

Table 1. Lennard-Jones Parameters Used in This Work

Ion and atoms	σ(A)	ε(kJ/mol)
Na^+ ion	1.776	20.8466
Al(=Si) atom	4.009	0.5336
O atom	2.890	0.6487

Table 2. Several Sets of Electrostatic Charges* Used in the Calculation of Distances of Na^+ Ions from the Center of Box and Interatomic Distances

Na^+	Al(=Si)	O_1	O_2	O_3
0.55	0.6081	−0.4431	−0.4473	−0.4380
0.6	0.5935	−0.4483	−0.4523	−0.4432
0.625	0.5861	−0.4509	−0.4548	−0.4458
0.65	0.5788	−0.4535	−0.4574	−0.4484
0.7	0.5641	−0.4586	−0.4624	−0.4536

* in electronic charge unit.

From the preliminary NVT MD simulations of dehydrated zeolite-A at 298.15 K using the LJ parameters in Table 1 and the several set of electrostatic charges in Table 2, the averaged distance of Na^+ ions from the center of α-cage (CB; the center of box) and interatomic distances are calculated and are compared with those obtained from the X-ray diffraction experiment of Pluth and Smith[2] in Table 3. Comparison of interatomic distance of Na_{II}-O_1 and Na_{II}-O_2 are omitted in Table 3 because of the vigoruous movement of Na_{II} type ions around the equipoints within the planes of 8-rings (discussed later). The overall agreement is quite good for all the values of q_{Na^+}, and among them, the result from the first set of electrostatic charges ($q_{Na^+}=0.55$) is believed as the best one, in view of the acuracy in the second figure of the distance of Na_{III} type ion from CB and the interatomic distances of Na-O. Even though the positions of Na^+ ions determined from X-ray crystallography are not exactly reproduced by the first set of electrostatic charges, since the overall picture is good enough, we have decided to use them in this and further studies of zeolite-A. In the MD simulation of dehydrated zeolite-A by Shin *et al.*,[28] they used the third set of electrostatic charges ($q_{Na^+}=0.625$).

More on the results of MD simulations at 298.15 K, Figure 1 shows the stereoplot, by ORTEP,[39] of 12 Na^+ ions and framework atoms in the α-cage of dehydrated zeolite-A at the end of 50,000 time steps run for average. The averaged x, y, and z coordinates of Na^+ ions and distances, r, from CB with the standard deviations are given in Table 4. Since Na(12) ion, Na_{III}, is near to Na(5) and Na(8) ions, these two ions are a little away from the α-cage to the corners of cubic box, when compared with the X-ray determined positions

Table 3. Calculated Distances of Na^+ Ions from the Center of Box and Interatomic Distances Using Several Sets of Electrostatic Charges

Distances	CB[a]-Na_I	CB-Na_{II}	CB-Na_{III}	Na_I-Na_{III}	Na_I-O_3	Na_I-O_2	Na_{II}-O_3	Na_{III}-O_1
Exp.	6.397[b]	6.267	5.001	3.700	2.323	2.915	2.590	2.611
0.55	6.455 ± .332	5.933 ± .237	5.033 ± .216	4.116 ± .261	2.342 ± .315	2.932 ± .308	2.569 ± .168	2.590 ± .267
0.6	6.465 ± .315	5.975 ± .207	5.109 ± .164	4.083 ± .238	2.337 ± .300	2.928 ± .294	2.519 ± .130	2.541 ± .180
0.625	6.467 ± .287	5.968 ± .236	5.132 ± .154	4.085 ± .196	2.338 ± .273	2.929 ± .267	2.504 ± .170	2.527 ± .123
0.65	6.471 ± .266	5.982 ± .225	5.164 ± .130	4.089 ± .261	2.336 ± .253	2.928 ± .248	2.484 ± .105	2.507 ± .154
0.7	6.479 ± .253	5.984 ± .191	5.206 ± .115	4.040 ± .180	2.329 ± .242	2.922 ± .237	2.458 ± .094	2.480 ± .140

[a]CB represents the center of box (or the center of α-cage). [b]in the unit of A.

Table 4. Average *x*, *y*, and *z* Coordinates of Na^+ Ions and Distances, *r*, from the Center of Box at 298.15 K for 50,000 Time Steps (10 ps)

Type	Na_I								Na_{II}			Na_{III}
No.	1	2	3	4	5	6	7	8	9	10	11	12
x	3.643 ± .170	−3.538 ± .176	3.509 ± .139	3.793 ± .252	−3.982 ± .170	3.566 ± .212	−3.584 ± .263	−4.014 ± .179	5.827 ± .215	0.896 ± .156	−0.086 ± .727	−3.561 ± .149
y	3.642 ± .173	3.521 ± .169	−3.520 ± .146	3.802 ± .261	−3.985 ± .174	−3.562 ± .213	3.581 ± .244	−4.013 ± .174	0.874 ± .139	−5.888 ± .179	0.019 ± .725	−3.557 ± .154
z	3.692 ± .166	3.585 ± .152	3.568 ± .129	−3.868 ± .252	4.040 ± .172	−3.659 ± .190	−3.667 ± .226	−4.098 ± .193	−0.557 ± .585	−0.504 ± .541	5.904 ± .170	0.028 ± .167
	6.337 ± .295	6.146 ± .286	6.118 ± .239	6.619 ± .441	6.933 ± .297	6.229 ± .354	6.254 ± .423	7.001 ± .315	5.918 ± .314	5.977 ± .269	5.905 ± .268	5.033 ± .216
r	6.455 ± .332									5.933 ± .237		5.033 ± .216

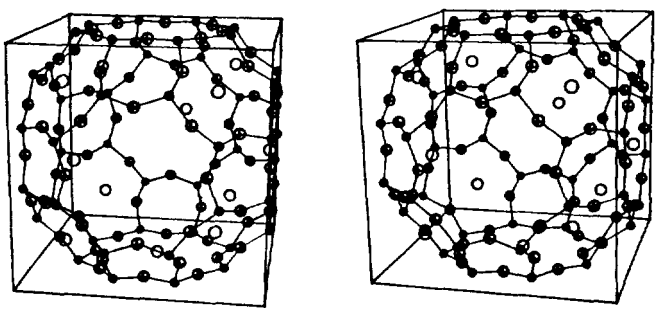

Figure 1. Stereoplot of 12 Na^+ ions in the α-cage of dehydrated zeolite-A at 298. 15 K at the end of 50,000 time steps run for average.

of Na_I type ions (± 3.693, coordinates and 6.397, distance from CB)[2]. In the stereoplot of Figure 1, these three Na^+ ions on a straight line along *z*-axis are shown in the left front of the view. The effect of the short distances between these ions can be seen as slightly higher potential energies of Na(5) and Na(8) ions compared with those of other Na_I type ions in Table 5, which indicates an unstable circumstance caused by the Na(12) ion, Na_{III}. Large values in the standard deviations of coordinates of Na_{II} type ions-Na(9), Na(10), and Na(11)-in Table 4 reflect the wanderings of these ions over the equipoints within the planes of 8-rings (cf. Figure 3 of Ref. 2). The big movement of Na_{II} type ions are apparently shown as large mean square displacements in Figure 3. Table 5, average potential energy of each Na^+ ion at 298.15 K, tells us that the Na^+ ions on sites I are most strongly bound to the framework atoms and the order of site selectivity is I>II>III, as expected.

Normalized velocity auto-correlation (VAC) functions and mean square displacements (MSD) of three types of Na^+ ions-Na_I, Na_{II}, and Na_{III}-are plotted in Figures 2 and 3. The VAC functions are oscillating continuously and not decaying rapidly to zero, which indicates random movings, back and

Table 5. Average Potential Energy (kJ/mol) of Each Na^+ Ion at 298.15 K for 50,000 Time Steps (10 ps)

Na_I								Na_{II}			Na_{III}
1	2	3	4	5	6	7	8	9	10	11	12
−161.6 ± 5.7	−165.1 ± 4.3	−165.5 ± 5.9	−160.9 ± 4.8	−154.4 ± 4.6	−164.3 ± 4.9	−168.1 ± 4.6	−155.4 ± 4.4	−115.1 ± 3.2	−117.7 ± 2.7	−119.2 ± 4.2	−102.3 ± 4.4
			−161.8 ± 6.2						−117.3 ± 4.4		−102.3 ± 4.4

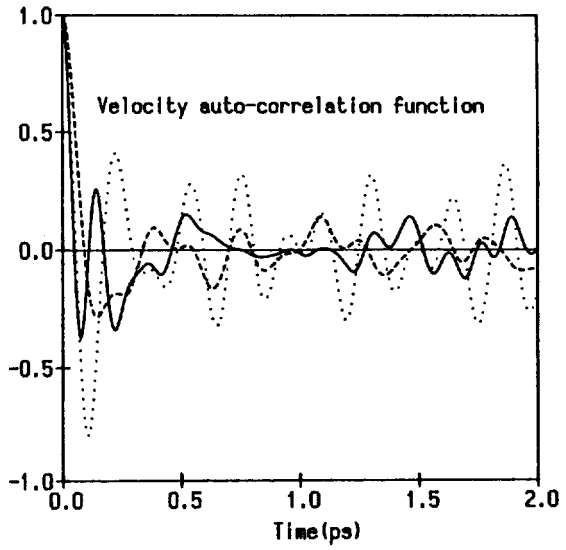

Figure 2. Normalized velocity auto-correlation functions of three types of Na^+ ions at 298.15 K. —— for Na_I, ----- for Na_{II}, and ····· for Na_{III}.

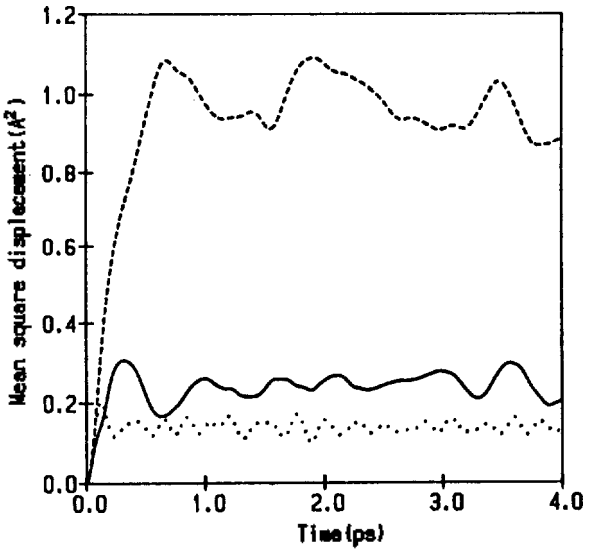

Figure 3. Mean square displacements of three types of Na^+ ions at 298.15 K —— for Na_I, ----- for Na_{II}, and ····· for Na_{III}.

forth, in closed cages with different speeds. The behavior of the MSD's is common; that of short, rapid increase and then that of slow, flat changes, which also indicates random moving in closed cages, but of different sizes. The three

Table 6. Self-diffusion Coefficients (10^{-5} cm^2/sec) of Three Types of Na^+ Ions Calculated from Velocity Auto-correlation Functions (VAC) and Mean Square Displacements (MSD)

Type	Na_I	Na_{II}	Na_{III}
VAC	0.60± 0.44	5.30± 2.02	5.29± 3.84
MSD	1.96± 0.62	3.75± 0.97	3.36± 0.30

peaks of the MSD of Na_{II} type ions may indicate their arriving at the other three equipoints started one of four equipoints. The self-diffusion coefficients of Na^+ ions, calculated from VAC using Eq. (15) and from MSD using Eq. (16), are gievn in Table 6:

$$D_s=\frac{1}{3}\int_0^\infty dt\langle v_i(t)\cdot v_i(0)\rangle \tag{15}$$

$$D_s=\lim_{t\to\infty}\frac{1}{6t}\langle|r_i(t)-r_i(0)|^2\rangle. \tag{16}$$

This table shows small motion of Na_I type ions and relatively big motion of Na_{II} and Na_{III} type ions as expected in Table 5. Disagreement between those values of D_s, calculated from two different routes, is inevitably due to the capture of Na^+ ions in zeolite-A, unlike in normal solutions. First, the failure of the Green-Kubo relation, Eq. (15), for self-diffusion coefficient comes from the bad-behaved, oscillating VAC, form which we can not obtain well-defined self-diffusion coefficients from the integration.[40,41] Second, the use of the corresponding Einstein relation, Eq. (16), fails because the calculated MSD's does not show straight lines at long times, at least 3 ps, and we can not obtain well-defined slopes of the MSD's (see Figure 3 of Ref. 42).

Lowering and raising of temperature are achieved by successive temperature increments of 50 K with 10,000 time steps run of equilibration after each increment. When the simulation temperature is lowered to 100.0 K, the positions and movements of Na^+ ions show almost the same patterns in the case of 298.15 K with smaller thermal motions and lower potential energies as shown in Table 7, average potential energy of each Na^+ ion at 100.0 K. For this reason, the discussion for the simulation result at 100.0 K is skipped.

However, the situation changes significantly when the temperature is raised to 600.0 K. First of all, more vigorous motion of Na^+ ions is fully expected escpecially the most unstable ion, Na_{III} type, which is Na(12) ion. As can be seen in Table 8, the changes of average potential energies of Na (12) and Na(5) ions in a sequence of enery 10,000 time steps

Table 7. Average Potential Energy (kJ/mol) of Each Na^+ Ion at 100.0 K for 60,000 Time Steps (12 ps)

Na_I								Na_{II}			Na_{III}
1	2	3	4	5	6	7	8	9	10	11	12
−170.0 ± 1.7	−170.6 ± 2.4	−172.5 ± 1.6	−162.1 ± 2.1	−153.8 ± 2.7	−166.1 ± 2.6	−165.2 ± 2.0	−154.7 ± 2.5	−118.4 ± 1.6	−119.0 ± 1.7	−124.3 ± 3.2	−105.5 ± 2.3
			−164.4 ± 7.0						−120.6 ± 3.5		−105.5 ± 2.3

Table 8. Change of Average Potential Energy (kJ/mol) of Each Na^+ Ion at 600.0 K. The Number in the Left Column Represents the Simulation Sequence of Every 10,000 Time Steps for Equilibration at 600.0 K

Type	Na_I								Na_{II}			Na_{III}
No.	1	2	3	4	5	6	7	8	9	10	11	12
1	−160.2 ± 4.6	−160.9 ± 8.4	−160.0 ± 6.2	−161.4 ± 5.2	−143.2 ± 8.9	−167.2 ± 5.4	−161.7 ± 6.4	−150.5 ± 7.9	−114.6 ± 2.8	−114.8 ± 3.2	−118.1 ± 3.5	−96.2 ± 6.0
2	−162.2 ± 6.3	−159.0 ± 8.3	−166.3 ± 4.4	−157.7 ± 8.0	−149.8 ± 6.3	−161.4 ± 6.3	−160.7 ± 6.8	−150.9 ± 7.2	−111.7 ± 5.7	−115.8 ± 3.6	−119.6 ± 4.2	−97.4 ± 7.0
3	−164.3 ± 4.7	−161.2 ± 6.3	−163.2 ± 5.6	−154.5 ± 10.4	−120.2 ± 24.1	−163.5 ± 4.8	−166.1 ± 4.8	−159.5 ± 9.0	−112.0 ± 6.6	−117.1 ± 3.6	−118.0 ± 3.9	−108.1 ± 15.1
4	−157.2 ± 8.2	−159.2 ± 6.1	−160.8 ± 5.3	−158.1 ± 6.5	−94.9 ± 8.5	−166.2 ± 5.5	−166.0 ± 5.7	−157.0 ± 12.1	−115.2 ± 4.1	−115.4 ± 4.0	−113.9 ± 4.9	−127.0 ± 13.0
5	−159.6 ± 6.2	−156.1 ± 7.2	−164.1 ± 7.4	−160.0 ± 4.6	−103.3 ± 8.0	−162.2 ± 5.8	−166.6 ± 5.4	−163.5 ± 5.2	−114.2 ± 5.8	−114.5 ± 5.2	−114.3 ± 4.6	−115.1 ± 10.7
6	−162.4 ± 5.7	−126.6 ± 19.7	−162.1 ± 6.8	−165.1 ± 5.4	−101.3 ± 13.7	−162.4 ± 5.7	−159.5 ± 12.2	−165.9 ± 5.6	−115.3 ± 5.1	−115.3 ± 4.0	−117.4 ± 4.2	−147.6 ± 25.4
7	−160.1 ± 5.8	−167.2 ± 4.1	−153.4 ± 7.3	−161.3 ± 5.6	−104.8 ± 11.8	−162.7 ± 5.5	−112.6 ± 9.5	−166.9 ± 6.2	−115.8 ± 4.9	−115.5 ± 4.4	−117.1 ± 4.0	−154.9 ± 10.2
8	−159.9 ± 6.4	−165.0 ± 4.3	−159.8 ± 4.2	−155.6 ± 7.9	−97.5 ± 10.2	−161.4 ± 8.3	−140.1 ± 17.4	−155.2 ± 9.2	−116.0 ± 4.0	−118.1 ± 2.8	−115.0 ± 4.1	−160.1 ± 6.7
9	−157.2 ± 7.2	−168.5 ± 3.9	−161.4 ± 5.1	−159.4 ± 9.9	−99.1 ± 13.2	−167.3 ± 5.5	−121.9 ± 14.4	−157.5 ± 8.4	−118.6 ± 4.2	−113.9 ± 4.7	−116.6 ± 4.1	−158.1 ± 6.9
10	−162.3 ± 5.5	−165.6 ± 6.6	−164.4 ± 4.2	−110.6 ± 18.7	−102.8 ± 17.5	−165.8 ± 4.7	−161.2 ± 8.5	−168.4 ± 4.8	−116.0 ± 6.7	−114.1 ± 5.6	−119.4 ± 3.5	−152.4 ± 7.8
11	−158.1 ± 6.4	−162.0 ± 6.8	−154.5 ± 5.3	−159.3 ± 6.9	−102.6 ± 16.3	−161.2 ± 5.6	−114.8 ± 15.7	−168.0 ± 4.7	−116.9 ± 3.5	−116.4 ± 3.0	−117.5 ± 4.3	−163.0 ± 7.3
12	−161.2 ± 4.6	−157.0 ± 7.8	−157.0 ± 4.7	−165.4 ± 4.2	−98.6 ± 11.9	−163.2 ± 5.1	−120.4 ± 10.0	−165.5 ± 6.1	−115.6 ± 4.3	−113.6 ± 4.2	−118.2 ± 4.2	−163.0 ± 6.2
13	−164.3 ± 5.0	−156.1 ± 7.4	−160.7 ± 5.9	−162.5 ± 4.4	−100.3 ± 11.3	−168.0 ± 5.3	−114.4 ± 11.3	−163.0 ± 5.7	−112.8 ± 5.0	−112.7 ± 4.4	−116.2 ± 3.9	−164.5 ± 5.6
14	−157.9 ± 6.6	−166.2 ± 5.3	−156.3 ± 7.5	−162.8 ± 5.4	−101.0 ± 11.4	−159.3 ± 9.5	−117.5 ± 14.7	−159.9 ± 8.2	−117.9 ± 4.6	−115.0 ± 3.3	−117-6 ± 4.1	−160.0 ± 6.9

run are dramatic. Na(12) ion is located at the middle position of two nearest Na_I type ions, namely Na(5) and Na(8) ions, at the begining of simulation for the system of 600.0 K as shown in Figure 1. But Figure 4, the stereoplot of 12 Na^+ ions at the end of 30,000 time steps (the 3rd run) after equilibration to 600.0 K, tells us that the most unstable ion, Na (12), pushes down Na(5) ion into the β-cage. It finally sits on the stable site I and becomes one of Na_I type ions as

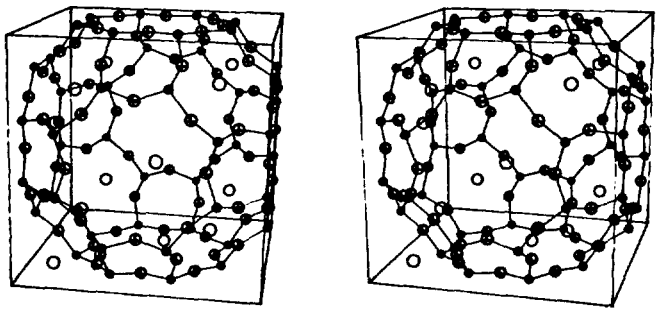

Figure 4. Stereoplot of 12 Na^+ ions in the α-cage of dehydrated zeolite-A at 600.0 K at the end of 30,000 time steps after equilibration.

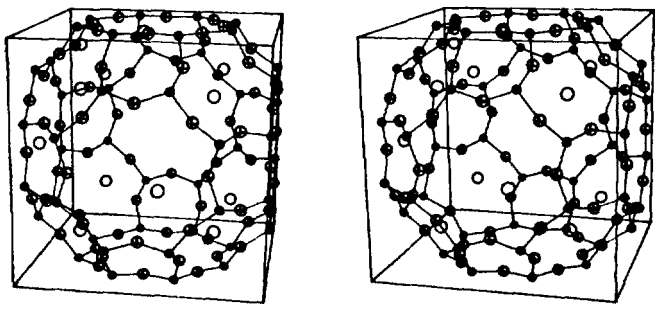

Figure 5. Stereoplot of 12 Na^+ ions in the α-cage of dehydrated zeolite-A at 600.0 K at the end of 70,000 time steps after equilibration.

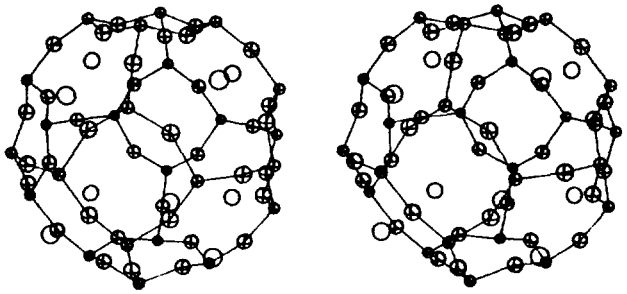

Figure 6. Stereoplot of 9 Na^+ ions in the β-cage of dehydrated zeolite-A at 600.0 K at the end of 70,000 time steps after equilibration.

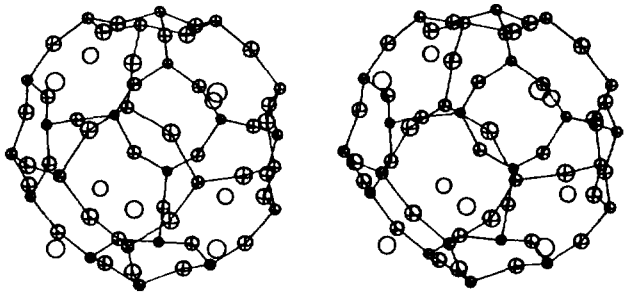

Figure 7. Stereoplot of 9 Na^+ ions in the β-cage of dehydrated zeolite-A at 600.0 K at the end of 100,000 time steps after equilibration.

shown in Figure 5, the stereoplot at the end of 70,000 time steps (the 7th run).

This pushing process, caused by temperature raising to 600.0 K, seems to end at the end of 50,000 time steps (10 ps). At the present moment, Na(5) ion is of neither Na_I nor Na_{III} type, but is captured in the β-cage and meta-stabilized at new type of site. Being kept by 8 Na_I ions on each center of 6-ring as shown in Figure 6, Na(5) ion wanders inside the β-cage and keeps colliding against one of the Na_I ions, for example, Na(2) ion during the 6th run, Na(4) ion during the 10th run, and Na(7) ion during the 7, 8, 9, 11, 12, 13, and 14th runs, which have somewhat higher average potential energies in Table 8. Figures 6 and 7 show stereoplots, centered at the β-cage, at the end of the 7th and 10th runs, respectively, in whcih Na(5) ion attacks Na(7) and Na (4) ions in turn. Na_{II} type ions-Na(9), Na(10), and Na(11)-have almost constant potential energies in Table 8 and probably remain near the starting points during the pushing process and even by the end of the 14th run. Average potential energies of Na(1), Na(3), Na(6), and Na(8) ions show also almost fixed values during 14,000 time steps, which means that these ions are kept near their starting positions and are not attcked by Na(5) ion.

This picture on the motion of Na^+ ions at 600.0 K is totally different from that of Shin *et al.*[28] in which Na_{III} type ion moves to one of the three neighboring 8-rings and at the same time the Na_{II} type ion, initially bound to site II (8-ring), moves to another neighboring site III, with Na_I type ions remaining near their starting points. After this "concerted transport process", the moved Na^+ ions sit on the equivalent sites to the initial sites, but exhibit actual bulk diffusions. In both of the two MD simulations which differ from each other in model parameters and in the treatment of long-range interaction, it turns out that Na_{III} type ion initiate the motion of the other ions. However, they predict that different target ions are attacked by the Na_{III} type ion. Which ion, Na_I or Na_{II} type, does the Na_{III} type ion attack more easily? The Na_{III} type ion is nearer to Na_I (3.7 A) than Na_{II} (5.3 A), but Na_I type ions are more stable than Na_{II} type ions as shown in the average potential energies, Tables 5, 7, and 8. We believe that high-temperature X-ray diffraction experiments can answer this question.

Concluding Remarks

In the present paper, we carried out molecular dynamic (MD) simulations of Na^+ ions in rigid dehydrated zeolite-A at 100.0, 298.15, and 600.0 K to study the structure and dynamics of Na^+ ions by using a simple Lennard-Jones potential plus Coulomb potential for the interactions between Na^+ ions and framework atoms at the microscopic level. The best-fitted set of electrostatic charges of Na^+ ions and framework atoms is chosen from the calculation of distances of Na^+ ions from the center of box and interatomic distances, and Ewald summation technique is used for the long-ranged character of Coulomb interaction. Based on the results obtained from our MD simulations, the following conclusions may be drawn: (1) At 298.15 K, the averaged x, y, and z coordinates of Na^+ ions are in good agreement with the X-ray determined positions[2] within statistical errors, and (2) from the calculated velocity auto-correlation (VAC) functions

and mean square displacements (MSD) of three types of Na^+ ions, the random movings of them in different types of closed cages is well-described and Na_I type ions are found to be less diffusive than Na_{II} and Na_{III}. (3) The structure and dynamics of Na^+ ions at 100.0 K show almost the same as those at 298.15 K with smaller thermal motions and lower potential energies. (4) At 600.0 K, the unstable Na_{III} type ion, located opposite the 4-ring, pushes down one of nearest Na_I ion into the β-cage and site on the stable site I, and (5) the captured ion in the β-cage wanders over and attacks one of 8 Na_I type ions, but fails in escaping from it. Finally, (6) the success of our MD simulation methods with Ewald summation technique promises the applications to further studies of zeolite-A system, for example, hydrated zeolite-A and Ca^{2+} ion-exchanged zeolite-A.

Acknowledgement. This work was supported by a research grant (901-0303-032-1) form the Korea Science and Engineering Foundation. The authors thank to the Computer Centers at Kyungsung University for the access to the MV/20000 system and at Pusan National University for the access to the Cyber 803 and Cyber 932.

References

1. D. W. Berk, "Zeolite Molecular Sieves" (Wiley, New York, 1974), p. 83.
2. J. J. Pluth and J. V. Smith, *J. Am. Chem. Soc.*, **102**, 4704 (1980).
3. G. W. Smith and R. Walls, *Mineral Mag.*, **38**, 72 (1971).
4. V. Gramlich and W. M. Meier, *Z. Kristallogr.*, **133**, 134 (1971).
5. A. G. Bezus, A. V. Kiselev, A. A. Lopatkin, and P. Q. Ku, *J. Chem. Soc., Faraday Trans. 2*, **74**, 367 (1978); A. V. Kiselev and P. Q. Du, *ibid.*, **77**, 1 (1981); *ibid.*, **77**, 17 (1981); A. V. Kiselev, A. A. Lopatkin, and A. Shulga, *Zeolites* **5**, 261 (1985).
6. P. A. Wright, J. M. Thomas, A. K. Cheetham, and A. K. Nowak, *Nature* **318**, 611 (1985).
7. A. K. Nowak, A. K. Cheetham, S. D. Pickett, and S. Ramdas, *Molecular Simulation*, **1**, 67 (1987).
8. S. Yashonath, J. M. Thomas, A. K. Nowak, and A. K. Cheetham, *Nature*, **331**, 601 (1988).
9. B. Smit and C. J. J. den Ouden, *J. Phys. Chem.*, **92**, 7169 (1988).
10. L. Leherte, D. P. Vercauteren, E. G. Derouane, and J. M. Andre, In Innovation in Zeolite Materials Science. "Studies in Surface Science and Catalyst" ed. by P. J. Grobet, W. J. Mortier, E. F. Vansant, and G. Schulz-Ekloff (Elsevier, Amsterdam, 1988), Vol. 37, p. 293.
11. P. Demontis, G. B. Suffritti, A. Alberti, S. Quartieri, E. S. Fois, and A. Gamba, *Gazz. Chim. Ital.*, **116**, 459 (1986).
12. P. Demontis, G. B. Suffritti, S. Quartieri, E. S. Fois, and A. Gamba, "Dynamics of Molecular Crystals" ed. by J. Lascombe (Elsevier, Amsterdam, 1987), p. 699.
13. P. Demontis, G. B. Suffritti, S. Quartieri, E. S. Fois, and A. Gamba, *Zeolites*, **7**, 522 (1987).
14. P. Demontis, G. B. Suffritti, S. Quartieri, E. S. Fois, and A. Gamba, *J. Phys. Chem.*, **92**, 867 (1988).
15. P. Demontis, E. S. Fois, G. B. Suffritti, and S. Quartieri, *J. Phys. Chem.*, **94**, 4329 (1990).
16. P. Demontis, G. B. Suffritti, S. Quartieri, A. Gamba, and E. S. Fois, *J. Chem. Soc., Faraday Trans.*, **87**, 1657 (1991).
17. E. Cohen de Lara, R. Kahn, and A. M. Goulary, *J. Chem. Phys.*, **90**, 7482 (1989).
18. E. Cohen de Lara and R. Kahn, *J. Phys.*, **42**, 1029 (1981).
19. S. Yashonath, P. Demontis, and M. L. Klein, *Chem. Phys. Lett.*, **153**, 551 (1988).
20. C. J. J. den Ouden, B. Smit, A. F. H. Wielers, R. A. Jackson, and A. K. Nowak, *Molecular Simulation*, **4**, 121 (1989).
21. S. Yashonath, P. Demontis, and M. L. Klein, *J. Phys. Chem.*, **93**, 5016 (1989).
22. L. Leherte, G. C. Lie, K. N. Swamy, E. Clementi, E. G. Derouane, and J. M. Andre, *Chem. Phys. Lett.*, **145**, 237 (1988).
23. L. Leherte, J. M. Andre, D. P. Vercauteren, and E. G. Derouane, *J. Molec. Catal.*, **54**, 426 (1989).
24. L. Leherte, J. M. Andre, E. G. Derouane, and D. P. Vercauteren, *Computers Chem.*, **15**, 273 (1991).
25. L. Leherte, J. M. Andre, E. G. Derouane, and D. P. Vercauteren, *J. Chem. Soc., Faraday Trans.*, **87**, 1959 (1991).
26. S. D. Pickett, A. K. Nowak, J. M. Thomas, B. K. Peterson, J. F. P. Swift, A. K. Cheetham, C. J. J. den Ouden, B. Smit, and M. F. M. Post, *J. Phys. Chem.*, **94**, 1233 (1990).
27. A. K. Nowak C. J. J. den Ouden, S. D. Pickett, B. Smith, A. K. Cheetham, M. F. M. Post, and J. M. Thomas, *J. Phys. Chem.*, **95**, 848 (1991).
28. J. M. Shin, K. T. No, and M. S. Jhon, *J. Phys. Chem.*, **92**, 4533 (1988).
29. S. W. de Leeuw, J. W. Perram, and E. R. Smith, *Proc. Roy. Soc. London* A373, 27 (1980).
30. N. Anastasiou and D. Fincham, *Comput. Phys. Commun.*, **25**, 159 (1982).
31. O.Steinhauser, *Mol. Phys.*, **45**, 335 (1982).
32. F. H. Stilinger and A. Rahman, *J. Chem. Phys.*, **60**, 1545 (1974).
33. M. Berkowitz and W. Wan, *J. Chem. Phys.*, **86**, 376 (1987).
34. E. Huheey, *J. Phys. Chem.*, **69**, 3284 (1965).
35. R. T. Sanderson, "Chemical Periodicity" (Reinhold, New York, 1960).
36. S. H. Lee, J. C. Rasaiah, and J. B. Hubbard, *J. Chem. Phys.*, **86**, 2383 (1987); *ibid.*, **85**, 5232 (1986).
37. K. F. Gauss, *J. Reine Angew. Math.*, **IV**, 232 (1829).
38. W. C. Gear, "Numerical Initial Value Problems in Ordinary Differential Equations" (McGraw-Hill, New York, 1965).
39. C. K. Johnson, ORTEP, Report ORNL-3794 (2nd revision, 1970), Oak Ridge National Laboratory, Oak Ridge, Tennessee, 1965.
40. C. B. Moon, G. K. Moon, and S. H. Lee., *Bull. Kor. Chem. Soc.*, **12**, 309 (1991).
41. S. H. Lee, G. K. Moon, and S. G. Choi., *Bull. Kor. Chem. Soc.*, **12**, 315 (1991).
42. A. Rahman, *Phys. Rev.*, **136**, 405 (1967).